Supplementary Material

Insight into the origin of photoreactivity of various well-defined Bi_2WO_6 crystals: exposed heterojunction-like surface and oxygen defect

Yongchao Ma[a], Qingzhi Liu[a], Qi Wang[a], Dan Qu[a], Jinsheng Shi[a]*

[a]Qingdao Agricultural University, Qingdao 266109, People's Republic of China

* Corresponding author:

Tel: +86-532-88030161; Fax: +86-532-86080213

E-mail address: jsshiqn@aliyun.com

Sample	X	E_g (eV)	E_{CB} (eV)	E_{VB} (eV)
Nanosheet-assembled microspheres	6.36	2.51	0.61	3.12
Nanoparticle-assembled microspheres	6.36	2.41	0.66	3.07
Single-crystalline nanosheets	6.36	2.51	0.61	3.12

Table S1 The valence band (VB) edge and the conduction band (CB) edge positions of Bi_2WO_6.

The valence band (VB) edge and the conduction band (CB) edge positions of the prepared Bi_2WO_6 can be calculated from the following formula:

$$E_{VB}=X-E^e+0.5E_g \qquad (1)$$

$$E_{CB}= E_{VB}- E_g \qquad (2)$$

where E_{VB} is the VB edge potential, E_{CB} is the CB edge potential, E_g is the band gap energy of the semiconductor, X is the electronegativity of the semiconductor that is the geometric mean of the elcetroegativity of the constituent atoms, E^e is the energy of free electrons on the hydrogen scale (about 4.5 eV). The X values of Bi_2WO_6 is 6.36 eV [1].

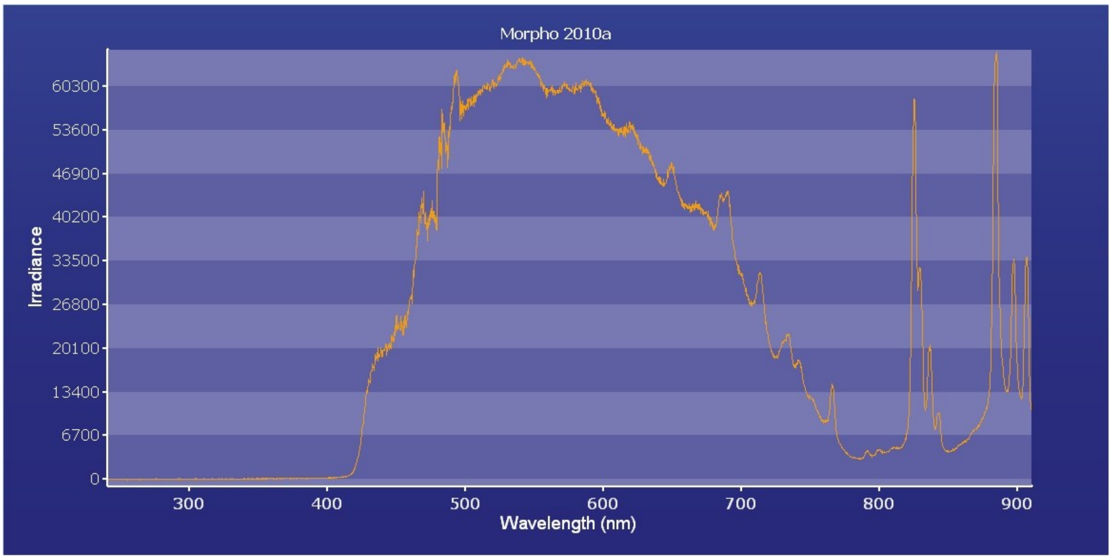

Fig. S1 Emission spectrum of the 300W Xe lamp with a 420 nm cutoff filter**.**

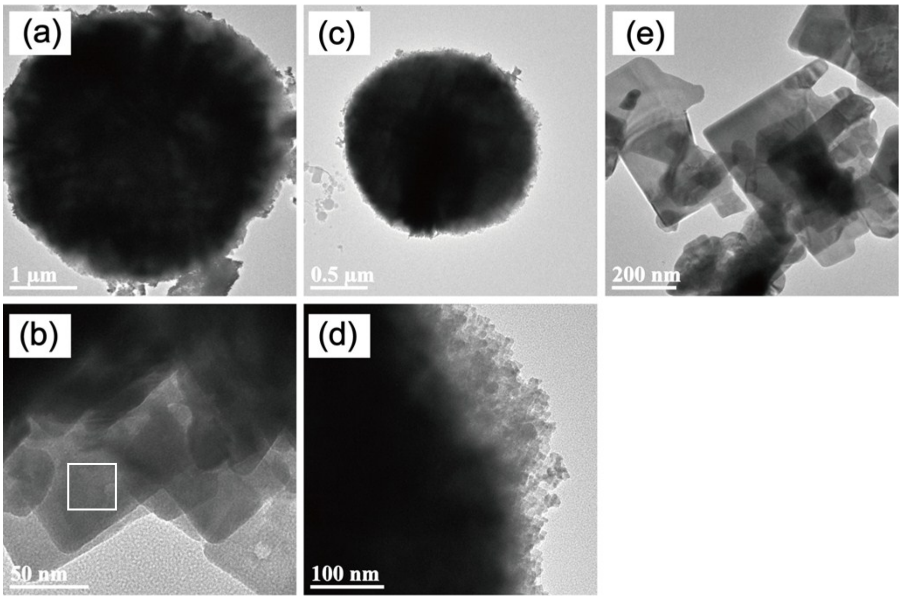

Fig. S2 TEM images of as-prepared Bi_2WO_6 samples: (a-b) nanosheet-assembled microspheres, (c-d) nanoparticle-assembled microspheres and (e) single-crystalline nanosheets.

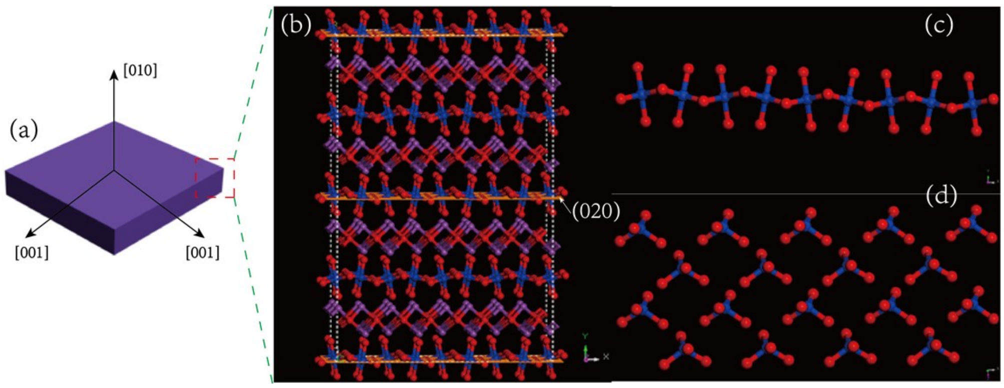

Fig. S3 (a) Schematic illustration of the crystal orientation of the nanosheets with exposed (020) facets. (b) The crystal structure of orthorhombic Bi_2WO_6. Atomic structure of the (020) facets: (c) side view and (d) top view. W, O and Bi atoms are represented as blue, red and yarrow spheres, respectively.

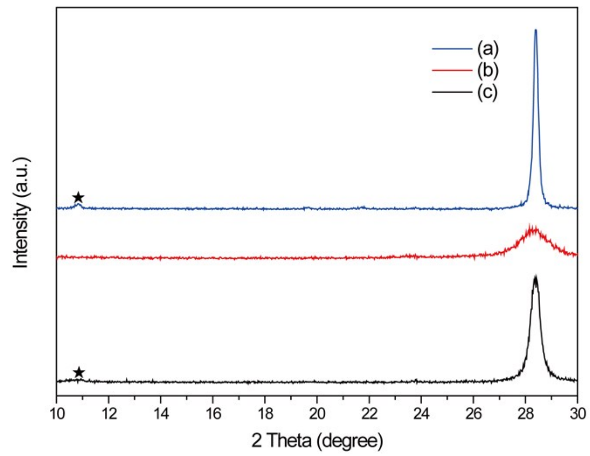

Fig. S4 Enlarged profile of the XRD patterns of the prepared Bi_2WO_6 samples between angles 10-30 °: (a) nanosheet-assembled microspheres, (b) nanoparticle-assembled microspheres and (c) single-crystalline nanosheets.

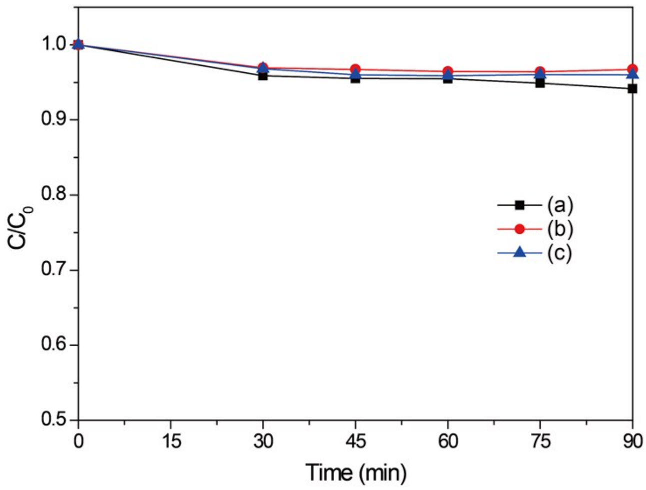

Fig. S5 Photocatalytic degradation of MO under visible light irradiation over various Bi_2WO_6 samples: (a) nanosheet-assembled microspheres, (b) nanoparticle-assembled microspheres and (c) single-crystalline nanosheets.

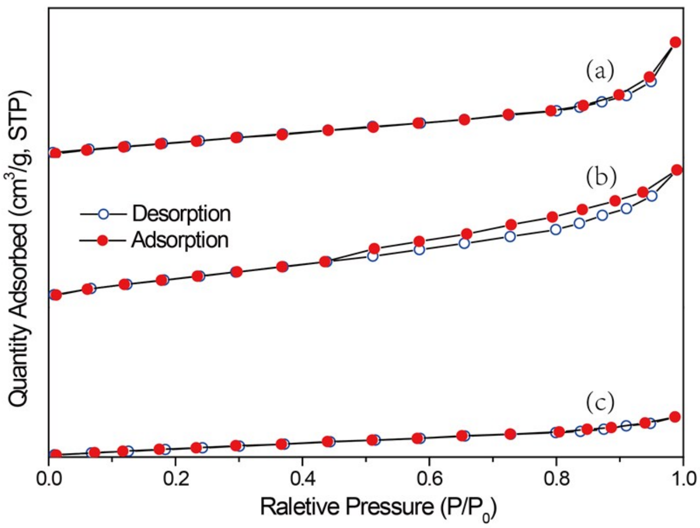

Fig. S6 N_2 absorption-desorption isotherms of the prepared Bi_2WO_6 samples: (a) nanosheet-assembled microspheres, (b) nanoparticle-assembled microspheres and (c) single-crystalline nanosheets.

Fig. S6 describes typical N_2 adsorption-desorption isotherms of the prepared samples. Both Bi_2WO_6 nanosheet-built microspheres and nanosheets showed a typical Ⅱ adsorption-desoprtion isotherms. In addition, the weak adsorption-desoprtion hysteresis demonstrated monolayer absorption. However, the nanoparticle-assembled microspheres displayed Ⅳ-type isotherm character, indicating the existence of mesopores. The specific surface areas of nanosheet-assembled microspheres, nanoparticle-assembled micropsheres and single-crystalline nanosheets are 26.97±1, 40.72±1 and 13.56±1 $m^2\ g^{-1}$, respectively.

Supplementary reference

1. L. Chen, H. Hua, Q. Yang and C. Hu, *Appl. Surf. Sci.*, 2015, 327, 62-67.